Initiation of linoleic acid autoxidation with ozone exposure in levitated aerosol particles

Marcel Müller[1,a], Marcel Reichmuth[1], and Ulrich K. Krieger[1]

[1]Institute for Atmospheric and Climate Science, ETH Zurich, Universitätstrasse 16, 8092 Zurich, Switzerland
[a]currently at: Institute of Biogeochemistry and Pollutant Dynamics, ETH Zurich, Universitätstrasse 16, 8092 Zurich, Switzerland

Correspondence: Marcel Müller (marcel.mueller@env.ethz.ch)

Abstract. When atmospheric aerosol particles undergo oxidation, their physico-chemical properties are altered, influenceing their environmental impact. Recent work has revealed that ozonolyis andautoxidation both contribute to the decay of linoleic acid. However, the observed linoleic acid decay rates could only be explained if the autoxidation induction period was shorter in experiments with ozone than without ozone. In this study, we investigate if linoleic acid autoxidation in levitated aerosol particles can be initiated by ozonolysis. Linoleic acid droplets were levitated in an electrodynamic balance, exposed to air with and without ozone, and subsequently analysed by mass spectrometry. Specifically, droplets were first exposed to air containing 39 or 619 ppb ozone for one hour, and thereafter, the gas phase was switched to air without ozone. The observed autoxidation rates were compared with reference experiments without the initial ozonolysis phase, the latter showing an extended induction period. These findings indicate that ozonolysis produces considerable radical concentrations leading to the observed shortening of the induction period. A comparison of the measurements to a simple one-compartment bulk reaction model was used to estimate the radical contribution from ozonolysis. To explain the observed shortening of the induction period, assuming that radicals are formed from the decomposition of linoleic acid oxidation products, a reaction rate constant for the decay of 5.1×10^{-8} s^{-1} is obtained. Studies under extreme conditions, such as highly elevated ozone concentrations, may overlook the role of the synergistic effects discussed here, which are only of importance at atmospherically relevant oxidant concentrations.

1 Introduction

Aerosol particles undergo ageing in the oxidizing atmosphere, which has an important effect on their role in influencing climate and air quality. Laboratory experiments on model systems, such as levitated particles, have been helpful to determine the impact of aerosol ageing on aerosol particles' physico-chemical properties (e.g., Krieger et al., 2012). Among other proxies, linoleic acid has been used in numerous studies as a model system to study the heterogeneous oxidation of (poly-)unsaturated fatty acids. For example, linoleic acid was found to undergo oxidation through reaction with ozone (Moise and Rudich, 2002; Thornberry and Abbatt, 2004; Broekhuizen, 2004; Hearn and Smith, 2004; Zeng et al., 2013; He et al., 2017; Woden et al., 2024), and because of its bis-allylic hydrogens it is also prone to autoxidation reactions with molecular oxygen (Lee and Chan, 2007; Chu et al., 2019). Therefore, linoleic acid is well-suited for studies on the competition between these two oxidation mechanisms and their synergistic effects, that may ultimately provide valuable insights into the chemical transformations that

25 aerosol particles undergo in the atmosphere.

In experiments investigating the influence of ozone concentration on linoleic acid oxidation, it was observed that the apparent ozone uptake coefficient depended on the ozone concentration (He et al., 2017; Chu et al., 2019). The higher uptake coefficients at lower ozone concentrations could be explained by a stronger relative contribution of autoxidation (Müller et al.,
30 2023). Hence, at atmospherically relevant ozone concentrations, the autoxidation with molecular oxygen contributes substantially to linoleic acid degradation. However, in our experiments without ozone, linoleic autoxidation only picked up speed after approximately 40 hours. Yet to explain the observed linoleic acid degradation, autoxidation would have to start earlier – essentially almost at the beginning of the experiment. These recent findings therefore suggest a synergistic effect where the presence of ozone shortens the autoxidation induction period. Radical formation as a result of ozonolysis, as reported in
35 studies of bulk samples (Goldstein et al., 1968; Pryor et al., 1976), could trigger the autoxidation. For example, Pryor (1994) suggested that approximately 10% of the ozone could react to form radicals. Several mechanisms have been proposed to explain radical formation from oxidation products, including from styrene peroxides (Mayo and Miller, 1956), methyl linoleate hydroperoxides (Morita and Tokita, 2006), linolenate hydroperoxides (Wang et al., 2025), and peroxides from α-pinene oxidation (Neuenschwander and Hermans, 2010, 2012). In particular, Kroll et al. (2002) proposed the formation of hydroxyl
40 radicals from Criegee intermediates, and Zeng et al. (2020) provided evidence for the formation of Criegee intermediates from OH-initiated lipid autoxidation.

In this study, we aim to investigate the influence of different oxidation schemes on the decay of linoleic acid in levitated droplets. Specifically, we focus on the impact of exposure to ozone prior to oxidation in an atmosphere without ozone, testing
45 both mild (39 ppb) and harsh (619 ppb) ozone concentrations. By examining these conditions, we test our previous hypothesis that ozonolysis can lead to radical formation and initiate autoxidation in levitated linoleic acid droplets. To contextualize our findings, we employ a simple one-compartment bulk reaction model to estimate the contribution of ozone-induced autoxidation initiation.

2 Instrumentation

50 The experiments on levitated linoleic acid particles were conducted with electrodynamic balance–mass spectrometry (EDB–MS). The setup used has been introduced previously (Müller et al., 2022). In brief, single linoleic acid droplets were produced from 10 wt-% methanol solutions, charged inductively, and injected into a quadrupolar electrodynamic trap flushed with nitrogen. The droplets were sized, and then exposed to specific gas phases for specific experiment durations. Subsequently, the particles were ejected into an evaporation unit and the produced gas plume was ionised and analysed with MS.

55

Linoleic acid ($\geq$ 99%, Sigma-Aldrich) and methanol (UHPLC for MS, Sigma-Aldrich) were used without further purification. Solutions were stored at temperatures below 6 °C and used within one week. Prior to the experiment, levitated droplets
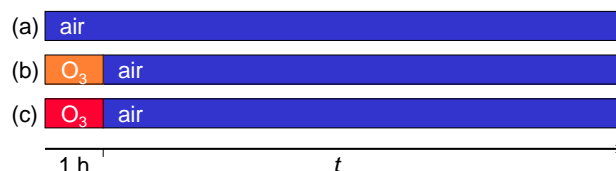
Figure 1. Schematic diagram of the different types of experiments conducted: An initial ozonolysis phase of 1 hour duration was applied in experiments (b) and (c), with 39 and 619 ppb ozone, respectively. Ozone was absent in experiments (a) denoted with 'air'.

were exposed to nitrogen for at least 15 minutes to ensure the complete evaporation of all methanol. The droplets were selected for comparable radii, ranging from 20.1 to 28.8 μm, with an average $\pm$ standard deviation of 24.1 $\pm$ 2.3 μm. The applied gas flux during ageing was 300 sccm, provided from a calibration ozone generator (Photometric O_3 Calibrator – Model 401, Advanced Pollution Instrumentation, USA) and the ozone concentration was measured with an electrochemical ozone sensor (Ozone Monitor BMT 932). The nominal concentrations during the initial ozonolysis were 750 and 50 ppb. A better estimate of the concentration in the particle trap was obtained from measurements of the gas outflow concentrations. For the two experiments (a) and (b) (see Fig. 1), the measured concentrations within one standard deviation were 619 $\pm$ 25 and 39 $\pm$ 17 ppb. Experiments were conducted at room temperature and under dry conditions (< 15% RH). The temperature of the evaporation unit was set to 190 °C (see Müller et al. (2022)). During MS analysis, a combination of nitrogen flows (1.5 l min^{-1} in total) was used, with 0.3 l min^{-1} applied to transfer the particle to the evaporation unit. Gas-phase analytes were ionised using a cold plasma dielectric barrier discharge ion source (SICRIT SC-30X Ionisation Set, Plasmion GmbH, Germany). Mass spectra were recorded using a triple quadrupole mass spectrometer (QTRAP 4500, AB Sciex LLC, USA) at unit resolution with a scan rate of 2000 Da s^{-1} for data ranges at m/z 84–86, 100–102, 120–122, 142–144, 156–160, 169–173, 184–188, 196–204, 208–212, and 276–283, with a 5 ms pause between mass ranges, resulting in a total scan time of 0.07 s. Mass spectra were integrated over 480 s and corrected for background.

Because of the destructive nature of the analysis, several experiments were conducted with droplets exposed to the same conditions but for different reaction times. Combining data from these experiments allows then to follow the course of the reaction. Experiments were carried out under three different conditions (see Figure 1). In experiments of type (a), droplets were exposed only to air without ozone. The corresponding data set partially includes data already published (Müller et al., 2023). For the other two types of experiments, (b) and (c), linoleic acid droplets were initially exposed to ozone-containing air for one hour, followed by an autoxidation phase in ozone-free air. To ensure comparability of data collected over an extended period (> 16 months), the data were normalised with respect to the sum of the two most prominent peaks in the spectrum at m/z 279 and 171 (see Appendix A).
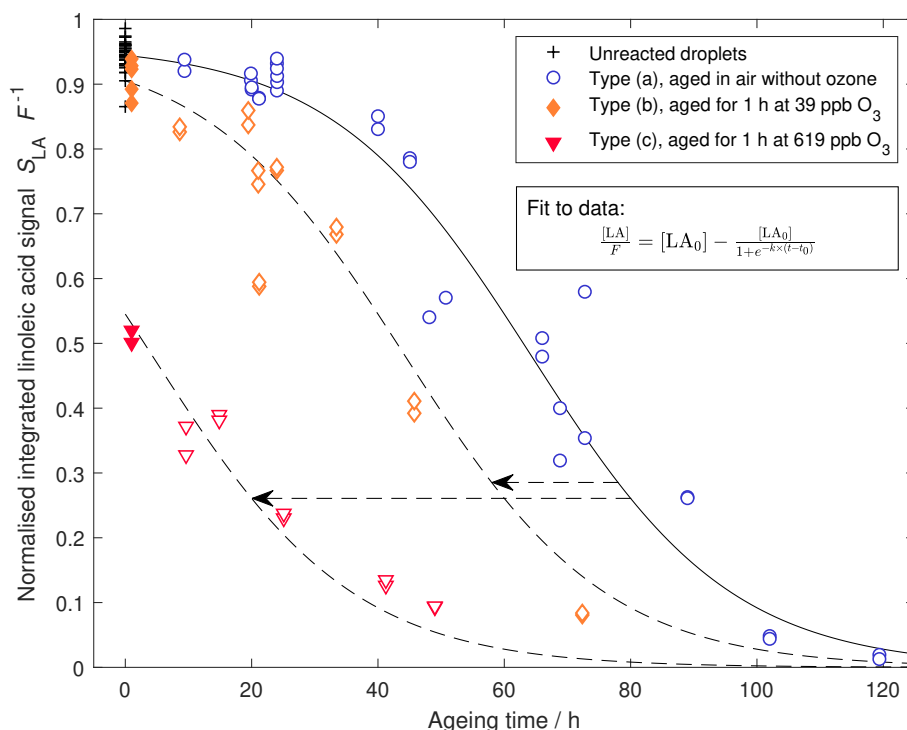
Figure 2. Linoleic acid decay with sigmoid fit. Filled symbols represent measurements after initial ozonolysis, and open symbols represent measurements after (subsequent) exposure to air without ozone. Due to the presence of product signal even at zero exposure, the normalised data does not equal one at zero exposure (see Appendix A). For the fit (black solid line), only the data from experiments without exposure to ozone exposure was used (+ and ○). The corresponding parameters are $[LA_0] = 0.961$, $k = 0.063$ h^{-1}, and $t_0 = 64.3$ h. Two additional sigmoid functions are shown with $t_0 = 44.3$ and 4.3 h, but otherwise identical parameters (dashed lines).

3 Results and discussion

3.1 Qualitative considerations

Data of the linoleic acid decay under the three different experimental types, (a), (b) and (c), are shown in Figure 2. As observed previously (Müller et al., 2023), the decay of linoleic acid in air reaches the fast radical chain reaction phase only after an initial induction period of approximately 40 hours. A sigmoid function is fitted to the data from experiments without ozone and displayed as black solid line in Figure 2.

The experiments of type (b) and (c) with initial exposure to ozone show a decrease in linoleic acid concentration during this first hour exposure, the extent of which depends on the ozone concentration. Oxidation with 619 ppb ozone resulted in a decrease of the linoleic acid signal by approximately 50%, whereas oxidation with 39 ppb ozone only led to a reduction of about 3%. This decay is consistent with the results of our previous study (Müller et al., 2023) and will not be discussed further

here. When looking at the autoxidation period past-ozonolysis, it is obvious that linoleic acid continues to decay rapidly after the exposure to 619 ppb ozone, without any noticeable induction period. For the 39 ppb ozone experiments, the ozone phase is still followed by an induction period, which appears to be shortened by approximately 20 hours. Two additional sigmoid functions (dashed lines), with the same parameters as in the fit for experiments of type (a) but shifted by 20 and 60 hours towards shorter induction periods, are shown to highlight the shortened induction period and the similarities of the oxidation decay in air after one hour exposure to 39 or 619 ppb ozone.

Comparing autoxidation rates after ozone-free induction and after ozonolysis allows us to extract the effect of ozonolysis on autoxidation qualitatively. The absence of an induction period in experiments with elevated ozone concentrations (619 ppb) implies a significant concentration of radicals resulting from ozonolysis, which drives the autoxidation after switching to ozone-free air. As the resulting decay rate is comparable to the maximum observed rate in the experiment (a) without ozone exposure, similar radical concentrations are expected in both cases. A similar, but less pronounced effect is observed after exposure to a lower ozone concentration of 39 ppb ozone. The fact that a clear shortening of the induction period is observable even in these experiments implies that the acceleration of autoxidation is highly relevant for atmospheric conditions. Consequently, these results also support our previous assumption (Müller et al., 2023) that an increase in the apparent ozone uptake coefficient towards lower ozone concentrations can be explained with the contribution of autoxidation, particularly because ozonolysis shortens the autoxidation induction period.

3.2 Model

To assess the influence of product decay on the radical concentration, we ran a one-compartment process model simulating the bulk chemistry of the linoleic acid system (see Figure 3 and Appendix B). In this model, both autoxidation and ozonolysis are resulting in a decay of linoleic acid. Ozonolysis of unsaturated fatty acids proceeds via the formation of a primary ozonide, which decays rapidly to give an aldehyde and a reactive Criegee intermediate (Criegee, 1975; Moise and Rudich, 2002; Lee and Chan, 2007). The latter are expected to undergo further reactions leading to dimers and oligomers (e.g., Vesna et al., 2009; Wang et al., 2016; Müller et al., 2022). The autoxidation of linoleic acid occurs mainly by abstraction of the bis-allylic hydrogen, leading to a pentadienyl radical. This can react with oxygen to form a peroxyl radical, which by hydrogen abstraction leads to hydroperoxide formation (Howard and Ingold, 1967; Chu et al., 2019; Müller et al., 2023). For simplicity, the dimers and oligomers from ozonolysis as well as the hydroperoxide products from autoxidation are treated by the model to be identical (termed 'Primary products' in Figure 3). The implications of this assumption are discussed below.

In the model, ozonolysis is implemented on the basis of a bulk ozone concentration according to Henry's law, and the ozonolysis rate is used as a fit parameter. The autoxidation is treated as a function of the radical concentration and to proceed independent of the oxygen concentration, as the hydrogen abstraction reaction is assumed to be rate-limiting (Maillard et al., 1983). For this, an autoxidation rate constant of $6.2 \times 10^1 \ \mathrm{M}^{-1}\mathrm{s}^{-1}$ and a radical-radical recombination rate of $4.4 \times 10^6 \ \mathrm{M}^{-1}\mathrm{s}^{-1}$ were taken from Howard and Ingold (1967). The radical concentration in experiments without ozone must initially increase
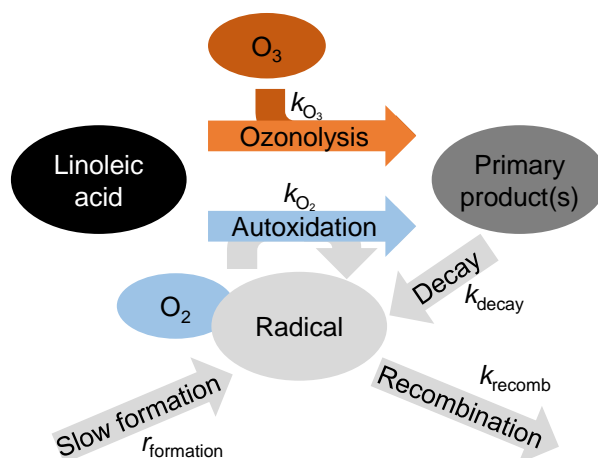
Figure 3. Depiction of the reaction scheme with the two linoleic acid decay mechanisms, ozonolysis and autoxidation, and the corresponding reaction rate constants.

because of a slow radical formation process, potentially due to impurities in the starting material that catalyse the oxidation with molecular oxygen. This process is assumed to happen in all experiments, but it is only of relevance in the absence of ozone. In the model, the slow radical formation is implemented with a constant source of radicals represented by a fit parame-
130   ter. Additionally, radicals are generated during the degradation of linoleic acid oxidation products, providing a mechanism for the acceleration of autoxidation and for an alternative initiation of autoxidation by ozonolysis. This unimolecular process is represented by another fit parameter. Potential reaction schemes for such a degradation have been suggested in the literature (Pryor et al., 1976; Kroll et al., 2002; Morita and Tokita, 2006; Neuenschwander and Hermans, 2012). This model, while a simplification, serves to estimate the impact of ozonolysis on autoxidation. The use of only one product species and the rep-
135   resentation of all possible product decay reactions with one reaction rate are supported by the observation that autoxidation rates post-ozonolysis under high ozone concentrations are similar to the autoxidation rates in experiments with no ozone (see discussion below). The used parameter values and the allowed ranges are provided in Table B1 in the appendix.

To infer the parameter values that best describe the measured linoleic acid decay, we used Markov chain Monte Carlo
140   (MCMC) simulations (see Appendix B). The corresponding findings are summarised in Table 1. While for the ozonolysis and for the product decay rate, single values can be extracted, the slow radical formation rate cannot be well constrained. This is because for values lower than approximately 6.3×10^{-10} M s^{-1}, the model is not sensitive to changes in the slow radical formation rate, as the total radical formation is dominated by the faster radical formation from autoxidation products. The slow radical formation would only have a significant impact on the outcome when it is assumed to be high enough to shorten the induction period in experiments without ozone, which would not be compatible with the observations. When the obtained pos-
145   terior mean values for the parameters are plugged into the model ($k_{O_3} = 7.3 \times 10^2$ M^{-1}s^{-1}, $r_{formation} = 1.1 \times 10^{-16}$ M s^{-1},

Table 1. Model parameter values for the global fit (fit parameters in the upper part and literature values in the lower part of the table). The 95% intervals, provided in brackets, are based on the MCMC sampling.

Parameter	Global fit
Ozonolysis rate constant k_{O_3} [M^{-1} s^{-1}]	7.3×10^2 ($5.9 \times 10^2, 8.9 \times 10^2$)
Slow radical formation rate $r_{formation}$ [M s^{-1}]	$\lesssim 6.3 \times 10^{-10}$
Product decay rate constant k_{decay} [s^{-1}]	5.1×10^{-8} ($4.4 \times 10^{-8}, 5.9 \times 10^{-8}$)
Autoxidation rate constant k_{O_2} [M^{-1} s^{-1}]	6.2×10^1 (Howard and Ingold, 1967)
Radical recombination rate constant k_{recomb} [M^{-1} s^{-1}]	4.4×10^6 (Howard and Ingold, 1967)
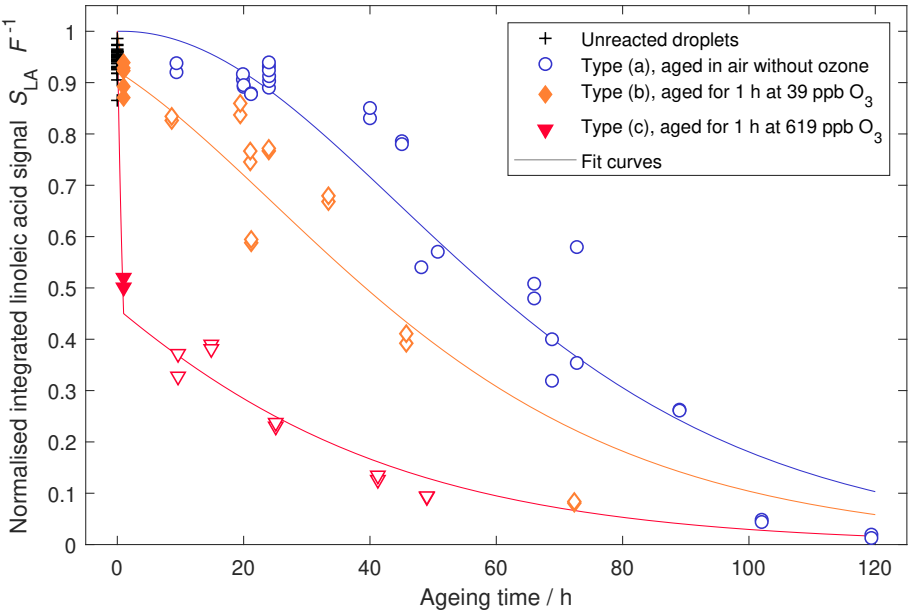
Figure 4. Experimental results and model curves resulting from the MCMC point estimate (posterior mean) for the model parameters as given in Table 1. Filled symbols represent measurements after initial ozonolysis, and open symbols represent measurements after (subsequent) exposure to air without ozone.

and $k_{decay} = 5.1 \times 10^{-8}$ s^{-1}), the model captures the data rather well (Figure 4). Notably, the model reflects the observed short-
ening of the induction period and the subsequent rapid decay phase for conditions with ozone, while resulting in a sigmoid
shape for ageing in the absence of ozone. However, the model cannot be brought into perfect agreement with all experimental
150 data. The obtained point estimates lead to a slight overestimation of the ozonolysis progress, and the linoleic acid concentra-
tions in the low ozone condition experiments are underestimated for most of the experiments. These deviations may be due
to the simplified model, which treats the potentially complex mixture of products and their ability to form radicals with one
single parameter. An estimation for the separated contributions to autoxidation can be obtained when the MCMC simulation is

run on a subset of the experimental data. For example, when using only the high-ozone data or only the data from experiments with no exposure to ozone. The corresponding simulations result in comparable product decay rates, which suggests that the different oxidation products do not differ substantially in their ability to cause autoxidation (see Table B2 in the appendix). In any case, it can be concluded that for our simple one-compartment bulk model, product decay rates on the order of 10^{-8} s^{-1} are required to reproduce the experimentally observed linoleic acid decay, namely a substantial shortening of the autoxidation induction period in the presence of low concentrations of ozone.

It should be noted that early oxidation products, such as slightly oxidised monomers, could strongly differ in terms of their decay and radical formation potential from later oxidation products that are more oxidised and potentially larger oligomers. Because of the thermal instability of dimers and oligomers, our instrumental setup does not allow us to distinguish the different types of products (Müller et al., 2023). Therefore, we were not able to capture differences in oxidation products, and their potentially different contributions to autoxidation are averaged in our approach presented here. The reaction system understanding could potentially be significantly improved if product formation was integrated in the analysis.

When applying the data presented here to atmospheric particles, it is important to take into account differences in both particle composition and size. In the atmosphere, particles are much smaller than in our experiment (Rose et al., 2021). If autoxidation is assumed to be a bulk process, variations in particle size would not directly affect the autoxidation process and therefore would not affect our results after ozonolysis. However, ozonolysis is significantly affected by particle size, as ozone uptake depends on the ratio of surface area to volume (Zeng et al., 2013). Consequently, it would be expected that the induction phase of autoxidation becomes even shorter for smaller particles, and the relative contribution of ozonolysis increases overall.

4   Conclusions

In this study, we investigated the effect of ozone on autoxidation in levitated linoleic acid particles. Our data support the hypothesis that under low ozone conditions, ozonolysis can contribute to the initiation of autoxidation in linoleic acid droplets. While the ozonolysis and autoxidation chemistry of linoleic acid is complex, our simple model is able to reproduce the main observed trends in linoleic acid decay while representing additional radical formation with one decay rate for oxidation products (estimated at 5.1×10^{-8} s^{-1}). More experiments with different detection techniques and other sequences of gas-phase exposures may help to disentangle the complex processes happening in linoleic acid droplets, and in atmospheric aerosol oxidation in general. Synergistic effects can play important roles at atmospherically relevant oxidant concentrations and may need to be considered, when investigating atmospheric processes and their impacts.

Data availability. The ageing times and the normalised integrated linoleic acid signal of the data points in Figures 2 and 4 are available online at https://doi.org/10.3929/ethz-b-000727019 (Müller et al., 2025).
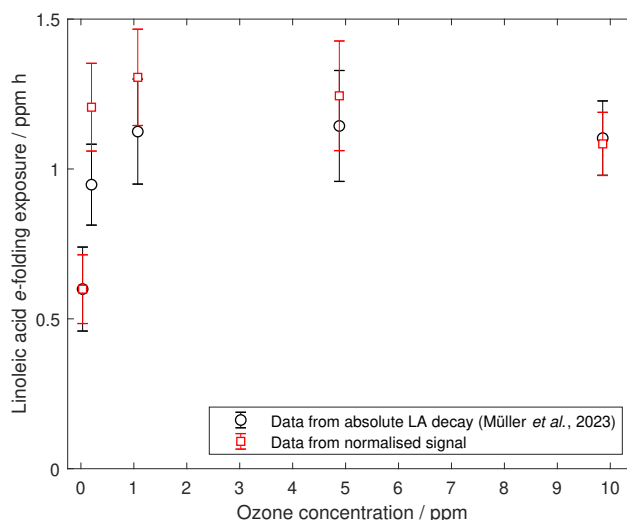
Figure A1. e-folding exposures of linoleic acid under different ozone concentrations. Original results are compared to results obtained from normalised integrated signals. The calculations of the e-folding exposures was carried out as published previously (Müller et al., 2023).

Appendix A: Normalisation

The experiments discussed in this study were carried out over an extended time span of over 16 months. To account for variability in evaporation, ionisation, and MS-sensitivity, the data was normalised using the peaks from linoleic acid (m/z 279) and the most prominent product peak (m/z 171) The linoleic acid fraction was then estimated by dividing the integrated linoleic acid signal by a normalisation divisor $F = \frac{S_{\mathrm{LA}}}{S_{\mathrm{LA},0}} + \frac{S_{171}}{S_{171,\infty}}$ with S_{LA} denoting the linoleic acid signal, S_{171} the product signal at m/z 171, $S_{\mathrm{LA},0}$ the average linoleic acid signal from all unreacted droplets, and $S_{171,\infty}$ the average signal at m/z 171 from all high-exposure experiments with less than 10% linoleic acid remaining. The values used in this study were $S_{\mathrm{LA},0} = 3.6 \times 10^5$ and $S_{171,\infty} = 2.2 \times 10^5$. Using this normalisation divisor also meant that the measured signal did not need to be corrected for droplet volume.

Normalising the linoleic acid peak was tested on the previously published data (Müller et al., 2023) and it resulted in comparable linoleic acid decay rates, see Figure A1.

Appendix B: Model

The following three reactions were used to simulate the chemistry in the droplets:

$$d/dt[\mathrm{LA}] = -k_{\mathrm{O}_2} \times [\mathrm{LA}] \times [\mathrm{Rad}] - k_{\mathrm{O}_3} \times [\mathrm{LA}] \times [\mathrm{O}_3] \tag{B1}$$

$$d/dt[\mathrm{Rad}] = r_{\mathrm{formation}} + k_{\mathrm{decay}} \times [\mathrm{Prod}] - 2k_{\mathrm{recomb}} \times [\mathrm{Rad}]^2 \tag{B2}$$

Table B1. Model parameters for the bulk model (fit parameters in the upper part and literature values in the lower part of the table).

Parameter	Allowed range	Reference
Ozonolysis rate constant k_{O_3} [M^{-1} s^{-1}]	$[10^2 - 10^4]$	Müller et al. (2023)[†]
Slow radical formation rate $r_{formation}$ [M s^{-1}]	$[10^{-20} - 10^{-1}]$[‡]	
Product decay rate constant k_{decay} [s^{-1}]	$[10^{-10} - 10^{-6}]$	
Autoxidation rate constant k_{O_2} [M^{-1} s^{-1}]	6.2×10^1	Howard and Ingold (1967)
Radical recombination rate constant k_{recomb} [M^{-1} s^{-1}]	4.4×10^6	Howard and Ingold (1967)

[†]Estimated from their linoleic acid decay at 10 ppm ozone and applying Henry's law as described in Appendix B of the current study.

[‡]On the lower side, the radical formation rate is limited by the rate required to generate at least one radical in a droplet of radius 25 μm within the first 40 h of the experiment, which corresponds to an $r_{formation}$ of approximately 3×10^{-20} M s^{-1}.

$$d/dt[\text{Prod}] = k_{O_2} \times [\text{LA}] \times [\text{Rad}] + k_{O_3} \times [\text{LA}] \times [\text{O}_3] - k_{decay} \times [\text{Prod}] \quad \text{(B3)}$$

The initial droplet composition was assumed to be pure linoleic acid, which deviates slightly from the normalised signal of un-reacted droplets that accounts for approximately 92% of the total signal. The ozone concentration in linoleic acid was estimated with a Henry's law constant for the corresponding solubility in oleic acid of 4.8×10^{-4} mol cm^{-3} atm^{-1} (Berkemeier et al., 2021). The simplification of the ozone uptake by using a uniform bulk ozone concentration and Henry's law is expected to be reflected in the resulting ozonolysis rate. However, fitting the reaction scheme to the observations still leads to the measured linoleic acid decay, and to the corresponding product and radical formation.

The compositional evolution over time was simulated with an ordinary differential equation solver in MATLAB R2019a with relative error tolerances of 1×10^{-6} and absolute error tolerances of 1×10^{-12}. The MCMC simulations were carried out using UQLab version 2.0 (Marelli and Sudret, 2014; Wagner et al., 2019). The fit parameters were sampled with log-uniform prior distribution using the ranges specified in Table B1. The allowed range for the ozonolysis and product decay rates were manually adjusted to capture more than the range required to reproduce the decay curve characteristics. For the experimentally determined values, a Gaussian discrepancy term was assumed with a relatively big standard error of 0.1 times the highest signal to be on the safe side in the event of any errors introduced from the standardisation calculation. The MCMC was run with 1×10^5 steps, of which the first 5×10^4 were discarded to avoid burn-in artefacts.

Author contributions. Funding was acquired by U. K. K. Experiments were conceptualised by M. M., and carried out by M. M. and M. R., the data was analysed by M. M. and M. R. The results were discussed by M. M., M. R., and U. K. K. The manuscript was written by M. M. and revised by M. R. and U. K. K.

Table B2. Inferred model parameter values (posterior mean) for the additional fits in comparison to the global fit. The 95% intervals, provided in brackets, are based on the MCMC sampling.

Parameter	Global fit	619 ppb ageing	Ozone-free air ageing
Ozonolysis rate constant k_{O_3} [M^{-1} s^{-1}]	7.3×10^2 $(5.9 \times 10^2, 8.9 \times 10^2)$	6.4×10^2 $(4.5 \times 10^2, 8.9 \times 10^2)$	–
Slow radical formation rate $r_{\text{formation}}$ [M s^{-1}]	$\lesssim 6.3 \times 10^{-10}$	$\lesssim 3.5 \times 10^{-7}$	$\lesssim 1.4 \times 10^{-9}$
Product decay rate constant k_{decay} [s^{-1}]	5.1×10^{-8} $(4.4 \times 10^{-8}, 5.9 \times 10^{-8})$	6.8×10^{-8} $(1.3 \times 10^{-8}, 2.0 \times 10^{-7})$	4.8×10^{-8} $(4.1 \times 10^{-8}, 5.6 \times 10^{-8})$

Competing interests. No competing interests are present.

Acknowledgements. This work was supported by ETH Research Grant ETH-03 17-2. Microsoft 365 Copilot was used to improve phrasing and paragraph structures. DeepL Write was used to improve phrasing. Both tools were accessed between December 2024 and February 2025.

References

225 Berkemeier, T., Mishra, A., Mattei, C., Huisman, A. J., Krieger, U. K., and Pöschl, U.: Ozonolysis of Oleic Acid Aerosol Revisited: Multiphase Chemical Kinetics and Reaction Mechanisms, ACS Earth and Space Chemistry, 5, 3313–3323, https://doi.org/10.1021/acsearthspacechem.1c00232, 2021.

Broekhuizen, K. E.: Formation of cloud condensation nuclei by oxidative processing: Unsaturated fatty acids, Journal of Geophysical Research, 109, D24 206, https://doi.org/10.1029/2004JD005298, 2004.

230 Chu, Y., Cheng, T. F., Gen, M., Chan, C. K., Lee, A. K. Y., and Chan, M. N.: Effect of Ozone Concentration and Relative Humidity on the Heterogeneous Oxidation of Linoleic Acid Particles by Ozone: An Insight into the Interchangeability of Ozone Concentration and Time, ACS Earth and Space Chemistry, 3, 779–788, https://doi.org/10.1021/acsearthspacechem.9b00002, 2019.

Criegee, R.: Mechanism of Ozonolysis, Angewandte Chemie International Edition in English, 14, 745–752, https://doi.org/10.1002/anie.197507451, 1975.

235 Goldstein, B. D., Balchum, O. J., Demopoulos, H. B., and Duke, P. S.: Electron Paramagnetic Resonance Spectroscopy, Archives of Environmental Health: An International Journal, 17, 46–49, https://doi.org/10.1080/00039896.1968.10665187, 1968.

He, X., Leng, C., Pang, S., and Zhang, Y.: Kinetics study of heterogeneous reactions of ozone with unsaturated fatty acid single droplets using micro-FTIR spectroscopy, RSC Advances, 7, 3204–3213, https://doi.org/10.1039/C6RA25255A, 2017.

Hearn, J. D. and Smith, G. D.: Kinetics and Product Studies for Ozonolysis Reactions of Organic Particles Using Aerosol CIMS, The Journal
240 of Physical Chemistry A, 108, 10 019–10 029, https://doi.org/10.1021/jp0404145, 2004.

Howard, J. A. and Ingold, K. U.: Absolute rate constants for hydrocarbon autoxidation. VI. Alkyl aromatic and olefinic hydrocarbons, Canadian Journal of Chemistry, 45, 793–802, https://doi.org/10.1139/v67-132, 1967.

Krieger, U. K., Marcolli, C., and Reid, J. P.: Exploring the complexity of aerosol particle properties and processes using single particle techniques, Chemical Society Reviews, 41, 6631–6662, https://doi.org/10.1039/c2cs35082c, 2012.

245 Kroll, J. H., Donahue, N. M., Cee, V. J., Demerjian, K. L., and Anderson, J. G.: Gas-Phase Ozonolysis of Alkenes: Formation of OH from Anti Carbonyl Oxides, Journal of the American Chemical Society, 124, 8518–8519, https://doi.org/10.1021/ja0266060, 2002.

Lee, A. K. Y. and Chan, C. K.: Heterogeneous Reactions of Linoleic Acid and Linolenic Acid Particles with Ozone: Reaction Pathways and Changes in Particle Mass, Hygroscopicity, and Morphology, The Journal of Physical Chemistry A, 111, 6285–6295, https://doi.org/10.1021/jp718121l, 2007.

250 Maillard, B., Ingold, K. U., and Scaiano, J. C.: Rate Constants for the Reactions of Free Radicals with Oxygen in Solution, Journal of the American Chemical Society, 105, 5095–5099, https://doi.org/10.1021/ja00353a039, 1983.

Marelli, S. and Sudret, B.: UQLab: A Framework for Uncertainty Quantification in Matlab, in: Vulnerability, Uncertainty, and Risk, pp. 2554–2563, American Society of Civil Engineers, Reston, VA, ISBN 9780784413609, https://doi.org/10.1061/9780784413609.257, 2014.

Mayo, F. R. and Miller, A. A.: Oxidation of Unsaturated Compounds. II. Reactions of Styrene Peroxide 1, Journal of the American Chemical
255 Society, 78, 1023–1034, https://doi.org/10.1021/ja01586a043, 1956.

Moise, T. and Rudich, Y.: Reactive Uptake of Ozone by Aerosol-Associated Unsaturated Fatty Acids: Kinetics, Mechanism, and Products, The Journal of Physical Chemistry A, 106, 6469–6476, https://doi.org/10.1021/jp025597e, 2002.

Morita, M. and Tokita, M.: The real radical generator other than main-product hydroperoxide in lipid autoxidation, Lipids, 41, 91–95, https://doi.org/10.1007/s11745-006-5075-9, 2006.

260   Müller, M., Mishra, A., Berkemeier, T., Hausammann, E., Peter, T., and Krieger, U. K.: Electrodynamic balance–mass spectrometry reveals
         impact of oxidant concentration on product composition in the ozonolysis of oleic acid, Physical Chemistry Chemical Physics, 24, 27 086–
         27 104, https://doi.org/10.1039/D2CP03289A, 2022.

       Müller, M., Stefanetti, F., and Krieger, U. K.: Oxidation pathways of linoleic acid revisited with electrodynamic balance–mass spectrometry,
         Environ. Sci.: Atmos., 3, 85–96, https://doi.org/10.1039/D2EA00127F, 2023.

265   Müller, M., Reichmuth, M., and Krieger, U. K.: Measurement report: Initiation of linoleic acid autoxidation with ozone exposure in levitated
         aerosol particles (Dataset), ETH Research Collection [data set], https://doi.org/10.3929/ethz-b-000727019, 2025.

       Neuenschwander, U. and Hermans, I.: Autoxidation of α-pinene at high oxygen pressure, Physical Chemistry Chemical Physics, 12, 10 542–
         10 549, https://doi.org/10.1039/c0cp00010h, 2010.

       Neuenschwander, U. and Hermans, I.: Thermal and catalytic formation of radicals during autoxidation, Journal of Catalysis, 287, 1–4,
270   https://doi.org/10.1016/j.jcat.2011.12.009, 2012.

       Pryor, W. A.: Mechanisms of radical formation from reactions of ozone with target molecules in the lung, Free Radical Biology and Medicine,
         17, 451–465, https://doi.org/10.1016/0891-5849(94)90172-4, 1994.

       Pryor, W. A., Stanley, J. P., Blair, E., and Cullen, G. B.: Autoxidation of Polyunsaturated Fatty Acids, Archives of Environmental Health: An
         International Journal, 31, 201–210, https://doi.org/10.1080/00039896.1976.10667220, 1976.

275   Rose, C., Collaud Coen, M., Andrews, E., Lin, Y., Bossert, I., Lund Myhre, C., Tuch, T., Wiedensohler, A., Fiebig, M., Aalto, P., Alastuey, A.,
         Alonso-Blanco, E., Andrade, M., Artinano, B., Arsov, T., Baltensperger, U., Bastian, S., Bath, O., Beukes, J. P., Brem, B. T., Bukowiecki,
         N., Casquero-Vera, J. A., Conil, S., Eleftheriadis, K., Favez, O., Flentje, H., Gini, M. I., Gomez-Moreno, F. J., Gysel-Beer, M., Hallar,
         A. G., Kalapov, I., Kalivitis, N., Kasper-Giebl, A., Keywood, M., Kim, J. E., Kim, S. W., Kristensson, A., Kulmala, M., Lihavainen,
         H., Lin, N. H., Lyamani, H., Marinoni, A., Martins Dos Santos, S., Mayol-Bracero, O. L., Meinhardt, F., Merkel, M., Metzger, J. M.,
280   Mihalopoulos, N., Ondracek, J., Pandolfi, M., Perez, N., Petaja, T., Petit, J. E., Picard, D., Pichon, J. M., Pont, V., Putaud, J. P., Reisen, F.,
         Sellegri, K., Sharma, S., Schauer, G., Sheridan, P., Sherman, J. P., Schwerin, A., Sohmer, R., Sorribas, M., Sun, J., Tulet, P., Vakkari, V.,
         Van Zyl, P. G., Velarde, F., Villani, P., Vratolis, S., Wagner, Z., Wang, S. H., Weinhold, K., Weller, R., Yela, M., Zdimal, V., and Laj, P.:
         Seasonality of the particle number concentration and size distribution: A global analysis retrieved from the network of Global Atmosphere
         Watch (GAW) near-surface observatories, Atmospheric Chemistry and Physics, 21, 17 185–17 223, https://doi.org/10.5194/acp-21-17185-
285   2021, 2021.

       Thornberry, T. and Abbatt, J. P. D.: Heterogeneous reaction of ozone with liquid unsaturated fatty acids: detailed kinetics and gas-phase
         product studies, Physical Chemistry Chemical Physics, 6, 84, https://doi.org/10.1039/b310149e, 2004.

       Vesna, O., Sax, M., Kalberer, M., Gaschen, A., and Ammann, M.: Product study of oleic acid ozonolysis as function of humidity, Atmospheric
         Environment, 43, 3662–3669, https://doi.org/10.1016/j.atmosenv.2009.04.047, 2009.

290   Wagner, P.-R., Nagel, J., Marelli, S., and Sudret, B.: UQLab user manual – Bayesian inversion for model calibration and validation, Tech.
         rep., Chair of Risk, Safety and Uncertainty Quantification, ETH Zurich, Switzerland, report n# UQLab-V1.3-113, 2019.

       Wang, M., Yao, L., Zheng, J., Wang, X., Chen, J., Yang, X., Worsnop, D. R., Donahue, N. M., and Wang, L.: Reactions of Atmospheric Par-
         ticulate Stabilized Criegee Intermediates Lead to High-Molecular-Weight Aerosol Components, Environmental Science and Technology,
         50, 5702–5710, https://doi.org/10.1021/acs.est.6b02114, 2016.

295   Wang, X., Fahy, W. D., Xie, L., Peng, H., and Abbatt, J. P. D.: Fast autoxidation of unsaturated lipid films on indoor surfaces, Nature
         Communications, 16, 1557, https://doi.org/10.1038/s41467-025-56802-0, 2025.

Woden, B., Su, Y., Skoda, M. W. A., Milsom, A., and Pfrang, C.: Oxidation by Ozone of Linoleic Acid Monolayers at the Air–Water Interface in Multi-Component Films at 21 °C and 3 °C., Faraday Discussions, 181, 3–7, https://doi.org/10.1039/D4FD00167B, 2024.

Zeng, G., Holladay, S., Langlois, D., Zhang, Y., and Liu, Y.: Kinetics of Heterogeneous Reaction of Ozone with Linoleic Acid and its
300   Dependence on Temperature, Physical State, RH, and Ozone Concentration, The Journal of Physical Chemistry A, 117, 1963–1974, https://doi.org/10.1021/jp308304n, 2013.

Zeng, M., Heine, N., and Wilson, K. R.: Evidence that criegee intermediates drive autoxidation in unsaturated lipids, Proceedings of the National Academy of Sciences of the United States of America, 117, 4486–4490, https://doi.org/10.1073/pnas.1920765117, 2020.